

$B \rightarrow X_s \gamma, X_s l^+ l^-$ Decays and Constraints on Mass Insertion Parameters in MSSM*

XIAO Zhen-Jun,[†] LI Feng-Ying, and ZOU Wen-Jun

Department of Physics and Institute of Theoretical Physics, Nanjing Normal University, Nanjing 210097, China

(Received January 10, 2006)

Abstract In this paper, we study the upper bounds on the mass insertion parameters $(\delta_{AB}^q)_{ij}$ in the minimal supersymmetric standard model. We found that the information from the measured branching ratio of $B \rightarrow X_s l^+ l^-$ decay can help us to improve the upper bounds on the mass insertions parameters $(\delta_{AB}^{u,d})_{3j,i3}$. Some regions allowed by the data of $\text{Br}(B \rightarrow X_s \gamma)$ are excluded by the requirement of an SM-like $C_{7\gamma}(m_b)$ imposed by the data of $\text{Br}(B \rightarrow X_s l^+ l^-)$.

PACS numbers: 13.25.Hw, 14.40.Nd, 12.60.Jv, 12.15.Ji

Key words: B meson decay, the minimal supersymmetric standard model, mass insertion

1 Introduction

As is well known, the radiative $B \rightarrow X_s \gamma$ decay and the semileptonic $B \rightarrow X_s l^+ l^-$ decay play an important role in the precision test of the standard model (SM) and the search for the new physics beyond the SM. Although no evidence of the new physics has been found now in experiments, one can put strong constraints on the parameter space of various new physics model from currently available data.

The minimal supersymmetric standard model (MSSM) is the general and most economical low-energy supersymmetric extension of the SM. In order to find the possible signals or hints of new physics from the date, various scenarios of the MSSM are proposed by imposing different constraints on it.^[1] Here, we use the phenomenological MSSM (pMSSM) model^[1] in our studies.

When calculating the new physics contributions to the flavor changing neutral current (FCNC) processes induced by the loop diagrams involving the new particles, one needs some kinds of model-independent parametrization of the FCNC SUSY contributions. The mass insertion approximation (MIA)^[2] is the best one of such kind of parametrization methods. In the MIA, one chooses a basis for the fermion and sfermion states, where all the couplings of these particles to neutral gaugino fields are flavor diagonal, and leaves all the sources of flavor violation inside the off-diagonal terms $(\Delta_{AB}^q)_{ij}$ of the sfermion mass matrix, i.e.,

$$(M_q^2)_{ij} = \tilde{m}^2 \delta_{ij} + (\Delta_{AB}^q)_{ij}, \quad (1)$$

where \tilde{m} is the averaged squark mass, A, B = (L, R), $q = u, d$, and the generation index $i, j = (1, 2, 3)$.

As long as the off-diagonal terms are much smaller than the averaged squark mass, the sfermion propagators can be expanded as a series in terms of $(\delta_{AB}^q)_{ij} =$

$(\Delta_{AB}^q)_{ij} / \tilde{m}^2$. Under the condition of $(\Delta_{AB}^q) \ll \tilde{m}^2$, one can just take the first term of this expansion and translate the relevant experimental measurements into upper bounds on these δ 's.

According to the helicity of the fermion partner, the squark mixings can be classified into left- or right-handed (L or R) pieces:

$$(\delta_{LL}^q)_{ij}, \quad (\delta_{RR}^q)_{ij}, \quad (\delta_{LR}^q)_{ij}, \quad (\delta_{RL}^q)_{ij}. \quad (2)$$

The LL and RR mixings represent the chirality conserving transitions in the left- and right-handed squarks, while the LR and RL mixings refer to the chirality flipping transitions. Up to now, many interesting works have been done to draw constraints on the parameter δ 's from the known data. The strong constraints on the mass insertion LL and RR, for example, are obtained from the measured ΔM_K , ΔM_{B_d} , and ϵ_K ,^[3] while the mass insertions in the LR and RL are constrained by the data of $\text{Br}(b \rightarrow s \gamma)$ ^[3,4] the ratio ϵ'/ϵ and the electric dipole moment (EDM) of the neutron, electron, and mercury atom.^[5]

Very recently, the possible SUSY corrections to the branching ratios and the CP-violating asymmetries of $B \rightarrow K \pi, K \eta',$ and ϕK decays have been studied, for example, in Refs. [4] ~ [6]. Here, the size and phase of the MIA parameters $(\delta_{AB}^q)_{3j,i3}$ with $i, j = (1, 2)$ play an impotent role in explaining those observed ‘‘puzzles’’ in B experiments or not.

The measured values of $\text{Br}(B \rightarrow X_s \gamma)$ and $\text{Br}(B \rightarrow X_s l^+ l^-)$ ^[7] agree perfectly with the SM predictions,^[8,9] which leads to strong constraints on various new physics models.^[10,11] From the well-measured $B \rightarrow X_s \gamma$ decays, the magnitude (but not the sign) of the Wilson coefficient $C_{7\gamma}(m_b)$ is strongly constrained. The sign of $C_{7\gamma}(m_b)$ and its absolute value, however, can be determined from the precision measurements of the $B \rightarrow X_s l^+ l^-$ decays.

*The project partly supported by National Natural Science Foundation of China under Grant Nos. 10275035 and 10575052 and the Research Foundation of Nanjing Normal University under Grant No. 214080A916

[†]Electronic address: xiaozhenjun@njnu.edu.cn

The latest Belle and BaBar measurements of the inclusive $B \rightarrow X_s l^+ l^-$ branching ratios indicated that the sign of $C_{7\gamma}(m_b)$ should be the same as the $C_{7\gamma}^{\text{SM}}(m_b)$.^[10] Therefore, when calculating the upper bounds of the mass insertions $(\delta_{AB}^q)_{3j,i3}$ in the MSSM, one should not only consider the constraint coming from the branching ratio of $B \rightarrow X_s \gamma$, but also the new information for the sign of $C_{7\gamma}(m_b)$ from the new measurements of $\text{Br}(B \rightarrow X_s l^+ l^-)$.

This paper is organized as follows. In Sec. 2, we show

the formulae needed to calculate the branching ratio of $B \rightarrow X_s \gamma$ decay at next-to-leading (NLO) order. The new physics contributions to the relevant Wilson coefficients are also given in this section. Then in Sec. 3, by comparing the theoretical predictions with the data of $B \rightarrow X_s \gamma$ and $B \rightarrow X_s l^+ l^-$ decay we update the upper bounds on those mass insertion parameters. We consider the cases of one mass insertion and two mass insertion approximation. Summary is given in the last section.

2 $\text{Br}(B \rightarrow X_s \gamma)$ in the SM and MSSM

2.1 $\text{Br}(B \rightarrow X_s \gamma)$ in the SM

In the SM, the effective Hamiltonian for $b \rightarrow s \gamma$ at scale $\mu \sim \mathcal{O}(m_b)$ reads^[12]

$$\mathcal{H}_{\text{eff}} = -\frac{G_F}{\sqrt{2}} V_{tb} V_{ts}^* \left[\sum_{i=1}^6 C_i(\mu) O_i(\mu) + C_{7\gamma}(\mu) O_{7\gamma}(\mu) + C_{8g}(\mu) O_{8g}(\mu) \right] + \text{h.c.}, \quad (3)$$

where $V_{tb} V_{ts}^*$ is the products of elements of the Cabbibo–Kabayashi–Maskawa (CKM) quark mixing matrix.^[13] The definitions and the explicit expressions of the operators O_i ($i = 1 \sim 6, 7\gamma, 8g$) and the corresponding Wilson coefficients C_i can be found in Ref. [12]. In the SM, the Wilson coefficients appeared in Eq. (3) are currently known at next-to-leading order (NLO) and can be found easily in Ref. [12].

At the lower energy scale $\mu_b \simeq \mathcal{O}(m_b)$, the Wilson coefficients at NLO level can be formally decomposed as follows:

$$C_i(\mu_b) = C_i^{(0)}(\mu_b) + \frac{\alpha_s(\mu_b)}{4\pi} C_i^{(1)}(\mu_b), \quad (4)$$

where $C_i^{(0)}$ and $C_i^{(1)}$ stand for the LO and NLO order part, respectively. Finally, the branching ratio $\text{Br}(B \rightarrow X_s \gamma)$, conventionally normalized to the semileptonic branching ratio $\text{Br}^{\text{exp}}(B \rightarrow X_c e \nu) = (10.64 \pm 0.23)\%$, is given by^[14,15]

$$\text{Br}(B \rightarrow X_s \gamma) = \text{Br}^{\text{exp}}(B \rightarrow X_c e \nu) \frac{|V_{ts}^* V_{tb}|^2}{|V_{cb}|^2} \cdot \frac{6\alpha_{em}}{\pi g(z) k(z)} [|\bar{D}|^2 + A + \Delta] \quad (5)$$

with

$$\begin{aligned} \bar{D}(\mu_b) &= C_{7\gamma}^{(0)}(\mu_b) + \frac{\alpha_s(\mu_b)}{4\pi} C_{7\gamma}^{(1)}(\mu_b) + \frac{\alpha_s(\mu_b)}{4\pi} \left\{ \sum_{i=1}^8 C_i^{(0)}(\mu_b) \left[r_i(z) + \gamma_{i7}^{(0)} \log \frac{m_b}{\mu_b} \right] - \frac{16}{3} C_{7\gamma}^{(0)}(\mu_b) \right\} \\ &= C_{7\gamma}(\mu_b) + V(\mu_b), \end{aligned} \quad (6)$$

$$A(\mu_b) = \frac{\alpha_s(\mu_b)}{\pi} \sum_{i,j=1;i \leq j}^8 \text{Re} \left\{ C_i^{0,\text{eff}}(\mu_b) \left[C_j^{0,\text{eff}}(\mu_b) \right]^* f_{ij} \right\}, \quad (7)$$

$$\Delta(\mu_b) = \frac{\delta_\gamma^{\text{NP}}}{m_b^2} \left| C_7^{0,\text{eff}}(\mu_b) \right|^2 + \frac{\delta_c^{\text{NP}}}{m_c^2} \text{Re} \left\{ \left[C_7^{0,\text{eff}}(\mu_b) \right]^* \left[C_2^{0,\text{eff}}(\mu_b) - \frac{1}{6} C_1^{0,\text{eff}}(\mu_b) \right] \right\} \quad (8)$$

with

$$\delta_\gamma^{\text{NP}} = \frac{\lambda_1}{2} - \frac{9}{2} \lambda_2, \quad \delta_c^{\text{NP}} = -\frac{\lambda_2}{9}, \quad (9)$$

where $z = (m_c^{\text{pole}}/m_b^{\text{pole}})^2$, $\lambda_1 = 0.5 \text{ GeV}^2$, $\lambda_2 = (m_{B^*}^2 - m_B^2)/4 = 0.12 \text{ GeV}^2$, and $m_b/2 \leq \mu_b \leq 2m_b$. The explicit expressions for the Wilson coefficients $C_i^{(0)}$, $C_i^{(1)}$, the anomalous dimension matrix γ , together with the functions $g(z)$, $k(z)$, $r_i(z)$ and $f_{ij}(\delta)$, can be found in Refs. [14] \sim [16]. The term $A(\mu_b)$ describes the correction from the bremsstrahlung process $b \rightarrow s \gamma g$, while the term Δ includes the non-perturbative $1/m_b$ ^[17] and $1/m_c$ ^[18] corrections.

Using above formulae and the input parameters as given in Table 1, we find the SM prediction for the branching ratio $\text{Br}(B \rightarrow X_s \gamma)$,

$$\text{Br}^{\text{NLO}}(B \rightarrow X_s \gamma) = (3.53 \pm 0.30) \times 10^{-4}, \quad (10)$$

where the main theoretical errors come from the uncertainties of the input parameters and have been added in quadrature. By using the same input parameters, it is easy to find the numerical values of $C_{7\gamma}(m_b)$, $V(m_b)$, $A(m_b)$, and

$\Delta(m_b)$ as defined in Eqs. (6) \sim (8),

$$\begin{aligned} C_{7\gamma}(m_b) &= -0.3052, & V(m_b) &= -0.0257 - 0.0156I, \\ A(m_b) &= 0.0033, & \Delta(m_b) &= -0.0010. \end{aligned} \quad (11)$$

One can see that it is the Wilson coefficient $C_{7\gamma}(m_b)$ that determines the branching ratio of $B \rightarrow X_s \gamma$ decay, while the last two terms $A(m_b)$ and $\Delta(m_b)$ are indeed very small.

Table 1 The input parameters entering the calculation of $\text{Br}(B \rightarrow X_s \gamma)$, their central values and errors. All masses are in unit of GeV. We use $G_F = 1.1664 \times 10^{-5}$ GeV.

M_W	M_Z	m_t	m_b	α^{-1}	$\alpha_s(M_Z)$
80.42	91.188	175 ± 5	4.8	137.036	0.118
BR _{SL}	m_c/m_b	μ_b	$\sin^2 \theta_W$	λ_1	λ_2
0.1064	0.29 ± 0.02	$4.8^{+4.8}_{-2.4}$	0.23	-0.5	0.12
A	λ	$\bar{\rho}$	$\bar{\eta}$	$ V_{tb}V_{ts}/V_{cb} ^2$	
0.854	0.2196	0.20 ± 0.09	0.33 ± 0.06	0.97 ± 0.01	

2.2 $\text{Br}(B \rightarrow X_s \gamma)$ in the MSSM

At the leading order, the one-loop diagrams involving internal line SUSY particles provide new physics contributions to the Wilson coefficients $C_{7\gamma}$, C_{8g} , as well as the Wilson coefficients $\tilde{C}_{7\gamma}$ and \tilde{C}_{8g} of the new operators $\tilde{O}_{7\gamma}$ and \tilde{O}_{8g} , which have the opposite chirality with $O_{7\gamma}$ and O_{8g} appeared in Eq. (3). In the SM, the contributions from chiral-flipped operators $\tilde{O}_{7\gamma,8g}$ are very small since they are strongly suppressed by a ratio $\mathcal{O}(m_s/m_b)$. In the MSSM, however, the contributions from the operators $\tilde{O}_{7\gamma}$ and \tilde{O}_{8g} do not have to be small in the SUSY models with non-universal A-terms.^[3,6,19]

At the one-loop level, there are four kinds of SUSY contributions to the $b \rightarrow s$ transition, depending on the virtual particles running in the penguin diagrams:

- (i) The charged Higgs boson H^\pm and up quarks u, c, t ;
- (ii) The charginos $\tilde{\chi}_{1,2}^\pm$ and the up squarks $\tilde{u}, \tilde{c}, \tilde{t}$;
- (iii) The neutralinos $\tilde{\chi}_{1,2,3,4}^0$ and the down squarks $\tilde{d}, \tilde{s}, \tilde{b}$;
- (iv) The gluinos \tilde{g} and the down squarks $\tilde{d}, \tilde{s}, \tilde{b}$.

In general, the Wilson coefficients at $\mu_w \sim M_W$ after the inclusion of various contributions can be expressed as

$$C_i(\mu_w) = C_i^{\text{SM}} + C_i^H + C_i^{\chi^+} + C_i^{\chi^0} + C_i^{\tilde{g}}, \quad (12)$$

where C_i^{SM} , C_i^H , $C_i^{\chi^+}$, $C_i^{\chi^0}$, and $C_i^{\tilde{g}}$ denote the Wilson coefficients induced by the penguin diagrams with the exchanges of the gauge boson W^\pm , the charged Higgs H^\pm , the chargino $\chi_{1,2}^\pm$, the neutralino $\chi_{1,2,3,4}^0$, and the gluino \tilde{g} , respectively.[‡]

In principle, the neutralino exchange diagrams involve the same mass insertions as the gluino ones, but they are strongly suppressed compared with the latter by roughly a ratio of $\alpha/\alpha_s \approx 0.06$. The charged Higgs contribution are proportional to the Yukawa couplings of light quarks and relevant only for a very small charged Higgs mass and very large $\tan \beta$. Therefore, We will concentrate on the chargino and gluino contributions only. The SUSY contributions to the Wilson coefficients $C_{7\gamma,8g}$ and $\tilde{C}_{7\gamma,8g}$ induced by various Feynman diagrams at the m_W scale have been calculated and collected, for example, in Refs. [3], [6], [19], and [20].

First, we consider the chargino contributions. As emphasized in Ref. [6], the chargino contributions induced by magnetic-penguin, and chromomagnetic-penguin diagrams depend on the up sector mass insertions $(\delta_{LL}^u)_{32,31}$ and $(\delta_{RL}^u)_{32,31}$, while the LR and RR contributions are suppressed by λ^2 or λ^3 , where $\lambda = 0.22$ is the Cabibbo mixing.

As for the mass spectrum of the squarks, the authors of Ref. [6] considered two cases: the case that all squarks have the same mass \tilde{m} and the case that the stop-right \tilde{t}_R is lighter than other squarks. But the numerical results show that the difference between these two cases are rather small. We therefor consider the first case only.

[‡]The parameter $\lambda_t = V_{tb}V_{ts}^*$ in Eq. (10) of Ref. [6] has been absorbed into the definition of $C_i^{\chi^+}$ and $C_i^{\tilde{g}}$ here.

At the high energy scale $\mu_w \approx M_W$, the chargino part of the Wilson coefficients, $C_{7\gamma}^X(m_w)$ and $C_{8g}^X(m_w)$, are of the form^[6]

$$C_{7\gamma}^X(m_w) = \lambda_t^{-1} \left\{ [(\delta_{LL}^u)_{32} + \lambda(\delta_{LL}^u)_{31}] R_{\gamma}^{LL} + [(\delta_{RL}^u)_{32} + \lambda(\delta_{RL}^u)_{31}] Y_t R_{\gamma}^{RL} \right\}, \quad (13)$$

$$C_{8g}^X(m_w) = \lambda_t^{-1} \left\{ [(\delta_{LL}^u)_{32} + \lambda(\delta_{LL}^u)_{31}] R_g^{LL} + [(\delta_{RL}^u)_{32} + \lambda(\delta_{RL}^u)_{31}] Y_t R_g^{RL} \right\} \quad (14)$$

with

$$\begin{aligned} R_{\gamma,g}^{LL} &= \sum_{i=1}^2 |V_{i1}|^2 x_{wi} P_{\gamma,g}^{LL}(x_i) - Y_b \sum_{i=1}^2 V_{i1} U_{i2} x_{wi} \frac{m_{\chi_i}}{m_b} P_{\gamma,g}^{LR}(x_i), \\ R_{\gamma,g}^{RL} &= - \sum_{i=1}^2 V_{i1} V_{i2}^* x_{wi} P_{\gamma,g}^{LL}(x_i), \\ P_{\gamma}^{LL}(x) &= \frac{x(-2-9x+18x^2-7x^3+3x(x^2-3)\log[x])}{9(1-x)^5}, \\ P_{\gamma}^{LR}(x) &= \frac{x(13-20x+7x^2+(6+4x-4x^2)\log[x])}{6(1-x)^4}, \\ P_g^{LL}(x) &= \frac{x(-1+9x+9x^2-17x^3+6x^2(3+x)\log[x])}{12(1-x)^5}, \\ P_g^{LR}(x) &= \frac{x(-1-4x+5x^2-2x(2+x)\log[x])}{2(1-x)^4}, \end{aligned} \quad (15)$$

where $Y_t = \sqrt{2}m_t/(v \sin \beta)$ and $Y_b = \sqrt{2}m_b\sqrt{1+\tan^2 \beta}/v$ are the Yukawa coupling of the top and bottom quark, $x_{wi} = m_w^2/m_{\chi_i}^2$, $x_i = m_{\chi_i}^2/\tilde{m}^2$, $\bar{x}_i = \tilde{m}^2/m_{\chi_i}^2$ with $i = (1, 2)$. Finally, U and V in Eq. (15) are the matrices that diagonalize chargino mass matrix, which is defined by

$$U^* M_{\tilde{\chi}^+} V^{-1} = \text{diag} \left(m_{\tilde{\chi}_1^+}, m_{\tilde{\chi}_2^+} \right) \quad (17)$$

with

$$M_{\tilde{\chi}^+} = \begin{pmatrix} M_2 & \sqrt{2}m_w \sin \beta \\ \sqrt{2}m_w \cos \beta & \mu \end{pmatrix}. \quad (18)$$

Here M_2 is the weak gaugino mass, μ is the supersymmetric Higgs mixing term, and $\tan \beta = v_2/v_1$ is the ratio of the vacuum expectation value (VEV) of the two-Higgs doublet. From the above functions one can obtain the following conclusions.

- (i) The second term in R_{γ}^{LL} and R_g^{LL} is enhanced by the large ratio $m_{\chi_i}/m_b \sim 30 \sim 100$ and therefore provides a large chargino contribution to both $C_{7\gamma}$ and C_{8g} .
- (ii) For a large $\tan \beta$, say around 30 to 50, the Yukawa coupling Y_b is also large and leads to a further enhancement to the LL terms in $C_{7\gamma}$ and C_{8g} .

In order to illustrate clearly the impact of the chargino contributions to $B \rightarrow X_s \gamma$ process, it is very useful to present the explicit dependence of the Wilson coefficients $C_{7\gamma}(M_W)$ and $C_{8g}(M_W)$ on the relevant mass insertions. For gaugino mass $M_2 = 200$ GeV, averaged squark mass $\tilde{m} = 500$ GeV, $\mu = 300$ GeV and $\tan \beta = 20$, we obtain numerically

$$C_{7\gamma}^X(M_W) = 0.411(\delta_{LL}^u)_{31} + 1.869(\delta_{LL}^u)_{32} + 0.002(\delta_{RL}^u)_{31} + 0.011(\delta_{RL}^u)_{32}, \quad (19)$$

$$C_{8g}^X(M_W) = 0.104(\delta_{LL}^u)_{31} + 0.475(\delta_{LL}^u)_{32} + 0.001(\delta_{RL}^u)_{31} + 0.004(\delta_{RL}^u)_{32}, \quad (20)$$

$$\tilde{C}_{7\gamma}^X(M_W) = 1.112(\delta_{RR}^u)_{31} + 5.062(\delta_{RR}^u)_{32} + 0.009(\delta_{LR}^u)_{31} + 0.042(\delta_{LR}^u)_{32}, \quad (21)$$

$$\tilde{C}_{8g}^X(M_W) = 0.507(\delta_{RR}^u)_{31} + 2.309(\delta_{RR}^u)_{32} + 0.006(\delta_{LR}^u)_{31} + 0.026(\delta_{LR}^u)_{32}. \quad (22)$$

It is evident that the MIA parameter $(\delta_{LL}^u)_{32}$ ($(\delta_{RR}^u)_{32}$) dominates the chargino contribution to $C_{7\gamma,8g}$ ($\tilde{C}_{7\gamma,8g}$). However, one should be careful with this contribution since it is also the main contribution to the $b \rightarrow s\gamma$, and stringent constraints on $(\delta_{LL}^u)_{32}$ are usually obtained, specially with large $\tan \beta$. Finally, as expected from Eq. (15), only LL contributions to $C_{7\gamma}^X$ and C_{8g}^X have strong dependence on the value of $\tan \beta$. With $\tan \beta = 40$, for instance, these contributions are enhanced by a factor 2, while the LR part of $C_{7\gamma}^X$ and C_{8g}^X are changing from the previous values by less than 2%.

Now let us turn to the gluino contributions in the $b \rightarrow s$ transition. Its contribution to $C_{7\gamma}$ and C_{8g} at scale μ_w is given by^[6]

$$C_{7\gamma}^{\tilde{g}} = \frac{8\alpha_s\pi}{9\sqrt{2}G_F\tilde{m}^2} \lambda_t^{-1} \left[(\delta_{LL}^d)_{23} M_3(x_{\tilde{g}}) + (\delta_{LR}^d)_{23} \frac{m_{\tilde{g}}}{m_b} M_1(x_{\tilde{g}}) \right], \quad (23)$$

$$C_{8g}^{\tilde{g}} = \frac{\alpha_s\pi}{\sqrt{2}G_F\tilde{m}^2} \lambda_t^{-1} \left[(\delta_{LL}^d)_{23} \left(\frac{1}{3} M_3(x_{\tilde{g}}) + 3M_4(x_{\tilde{g}}) \right) + (\delta_{LR}^d)_{23} \frac{m_{\tilde{g}}}{m_b} \left(\frac{1}{3} M_1(x_{\tilde{g}}) + 3M_2(x_{\tilde{g}}) \right) \right], \quad (24)$$

$$\tilde{C}_{7\gamma}^{\tilde{g}} = \frac{8\alpha_s\pi}{9\sqrt{2}G_F\tilde{m}^2} \lambda_t^{-1} \left[(\delta_{RR}^d)_{23} M_3(x_{\tilde{g}}) + (\delta_{RL}^d)_{23} \frac{m_{\tilde{g}}}{m_b} M_1(x_{\tilde{g}}) \right], \quad (25)$$

$$\tilde{C}_{8g}^{\tilde{g}} = \frac{\alpha_s\pi}{\sqrt{2}G_F\tilde{m}^2} \lambda_t^{-1} \left[(\delta_{RR}^d)_{23} \left(\frac{1}{3} M_3(x_{\tilde{g}}) + 3M_4(x_{\tilde{g}}) \right) + (\delta_{RL}^d)_{23} \frac{m_{\tilde{g}}}{m_b} \left(\frac{1}{3} M_1(x_{\tilde{g}}) + 3M_2(x_{\tilde{g}}) \right) \right], \quad (26)$$

where $x_{\tilde{g}} = m_{\tilde{g}}^2/\tilde{m}^2$ and the functions $M_i(x)$ can be found in Ref. [6].

Here in order to understand the impact of the gluino contributions to the branching ratio of $b \rightarrow s\gamma$, we also present the explicit dependence of the Wilson coefficients $C_{7\gamma,8g}$ on the relevant mass insertions. For $\tilde{m} = 500$ GeV, and $x = 1$, we obtain

$$C_{7\gamma}^{\tilde{g}}(M_W) = -0.049(\delta_{LL}^d)_{23} - 17.168(\delta_{LR}^d)_{23}, \quad (27)$$

$$C_{8g}^{\tilde{g}}(M_W) = -0.130(\delta_{LL}^d)_{23} - 64.379(\delta_{LR}^d)_{23}, \quad (28)$$

$$\tilde{C}_{7\gamma}^{\tilde{g}}(M_W) = -0.049(\delta_{RR}^d)_{23} - 17.168(\delta_{RL}^d)_{23}, \quad (29)$$

$$\tilde{C}_{8g}^{\tilde{g}}(M_W) \simeq -0.130(\delta_{RR}^d)_{23} - 64.379(\delta_{RL}^d)_{23}. \quad (30)$$

It is easy to see that the MIA parameter $(\delta_{LR}^d)_{23}$ ($(\delta_{RL}^d)_{23}$) dominates the gluino contribution to $C_{7\gamma,8g}^{\tilde{g}}$ ($\tilde{C}_{7\gamma,8g}^{\tilde{g}}$).

After the inclusion of the chargino and gluino contributions, the total Wilson coefficients $C_{7\gamma}(M_W)$ and $C_{8g}(M_W)$ can be written as

$$C_{7\gamma(8g)}(M_W) = C_{7\gamma(8g)}^{\text{SM}}(M_W) + C_{7\gamma(8g)}^{\chi}(M_W) + C_{7\gamma(8g)}^{\tilde{g}}(M_W), \quad (31)$$

$$\tilde{C}_{7\gamma(8g)}(M_W) = \tilde{C}_{7\gamma(8g)}^{\chi}(M_W) + \tilde{C}_{7\gamma(8g)}^{\tilde{g}}(M_W). \quad (32)$$

Since the heavy SUSY particles have been integrated out at the scale $\mu_w = M_W$, the QCD running of the the Wilson coefficients $C_i(M_W)$ down to the lower energy scale $\mu_b = \mathcal{O}(m_b)$ after including the new physics contributions is the same as in the SM.

3 Constraints on Mass Insertion Parameters

In this section, we will update the constraints on the mass insertion parameters $(\delta_{AB}^{u,d})_{ij}$ by considering the data of the branching ratios for the $B \rightarrow X_s \gamma$ decay and the semileptonic $B \rightarrow X_s l^+ l^-$ decay.

For $B \rightarrow X_s \gamma$ decay, the new world average as given by heavy flavor averaging group (HFAG)^[7] is

$$\text{Br}(B \rightarrow X_s \gamma) = (3.39_{-0.27}^{+0.30}) \times 10^{-4}, \quad (33)$$

where the error is generally treated as 1σ error. From this result the following bounds (at 3σ level) are obtained,

$$2.53 \times 10^{-4} < \text{Br}(B \rightarrow X_s \gamma) < 4.34 \times 10^{-4}. \quad (34)$$

Here the experimental error at 3σ level has been added in quadrature with the theoretical error in the SM as given in Eq. (10). From the bounds in Eq. (34), the magnitude (but not the sign) of the Wilson coefficient $C_{7\gamma}(m_b)$ can be strongly constrained. In the SM, the allowed ranges for a real $C_{7\gamma}(m_b)$ are found to be

$$-0.360 \leq C_{7\gamma}(m_b) \leq -0.248, \quad (35)$$

$$0.454 \leq C_{7\gamma}(m_b) \leq 0.564. \quad (36)$$

But the second range, where $C_{7\gamma}(m_b)$ is positive in sign, is strongly disfavored by the measured branching ratios of $B \rightarrow X_s l^+ l^-$ decays.^[10]

By using $M_2 = 200$ GeV, $\tilde{m} = 500$ GeV, $\mu = 300$ GeV, $\tan\beta = 20$, and $x_{\tilde{g}} = 1$, we find the numerical result for the Wilson coefficient $C_{7\gamma}(m_b)$ after the inclusion of new physics contributions from chargino and gluino penguins,

$$\begin{aligned} C_{7\gamma}(m_b) = & -0.3052 - 0.045(\delta_{LL}^d)_{23} + 0.284(\delta_{LL}^u)_{31} + 1.295(\delta_{LL}^u)_{32} \\ & - 17.41(\delta_{LR}^d)_{23} - 0.002(\delta_{RL}^u)_{31} + 0.008(\delta_{RL}^u)_{32}, \end{aligned} \quad (37)$$

where the first term is the $C_{7\gamma}^{\text{SM}}(m_b)$ at the NLO level, other terms represent the new physics contributions considered here. Using the same input parameters, the chiral flipped part $\tilde{C}_{7\gamma}(m_b)$ is found to be

$$\begin{aligned} \tilde{C}_{7\gamma}(m_b) = & -0.045(\delta_{\text{RR}}^d)_{23} + 0.007(\delta_{\text{RR}}^u)_{31} + 0.030(\delta_{\text{RR}}^u)_{32} \\ & - 17.41(\delta_{\text{RL}}^d)_{23} + 0.791(\delta_{\text{LR}}^u)_{31} + 3.601(\delta_{\text{LR}}^u)_{32}. \end{aligned} \quad (38)$$

From Eqs. (37) and (38) one can obtain the following conclusions:

(i) For the MIA parameters $(\delta_{\text{RL}}^u)_{31,32}$, $(\delta_{\text{LL}}^d)_{23}$, $(\delta_{\text{RR}}^u)_{31,32}$, and $(\delta_{\text{RR}}^d)_{23}$, there is no real constraint[§] can be derived from the data of $B \rightarrow X_s \gamma$ and $B \rightarrow X_s l^+ l^-$ because of the tiny coefficients of these terms. We set these parameters zero in the following analysis.

(ii) The MIA parameters $(\delta_{\text{LR}}^d)_{23}$ and $(\delta_{\text{LL}}^u)_{31,32}$ ($(\delta_{\text{LR}}^u)_{31,32}$, and $(\delta_{\text{RL}}^u)_{23}$) dominate the new physics contributions to $C_{7\gamma}(m_b)$ ($\tilde{C}_{7\gamma}(m_b)$).

When we take the new physics contributions into account, the branching ratio of $B \rightarrow X_s \gamma$ decay can be written as

$$\text{Br}(B \rightarrow X_s \gamma) = \text{Br}^{\text{exp}}(B \rightarrow X_c e \nu) \frac{|V_{ts}^* V_{tb}|^2}{|V_{cb}|^2} \cdot \frac{6\alpha_{em}}{\pi g(z)k(z)} \left[|C_{7\gamma}(\mu_b) + V(\mu_b)|^2 + A(\mu_b) + \Delta(\mu_b) + \left| \tilde{C}_{7\gamma}(\mu_b) \right|^2 \right], \quad (39)$$

where $C_{7\gamma}(\mu_b)$ includes the SM and the SUSY contributions as shown in Eq. (37), while the last term refers to the new physics contribution coming from the chiral-flipped operators $\tilde{O}_{7\gamma}$ and \tilde{O}_{8g} . For the functions $V(\mu_b)$, $A(\mu_b)$, and $\Delta(\mu_b)$ in Eq. (39), the possible new physics contributions to terms $A(\mu_b)$ and $\Delta(\mu_b)$ are very small and will be neglected in the following numerical calculations.

Since the gluino and the chargino contributions are given in terms of the MIA parameters of the up and down squark sectors, they are, in principle, independent and could have constructive or destructive interference between themselves or with the SM contribution. If we consider all MIA parameters in Eqs. (37) and (38) simultaneously, no meaningful constraint can be obtained indeed. So we consider the cases of one mass insertion and two-mass insertion only:

- (i) One mass insertion: the SM contribution and one non-zero MIA parameter are taken into account;
- (ii) Two mass insertion: the SM contribution and two non-zero MIA parameters are taken into account.

3.1 One Mass Insertion: Gluino Contributions

We now consider the case of only one mass insertion parameter is non-zero at a time. The MIA parameters in general may be complex and can be written as

$$(\delta_{\text{LR}}^q)_{ij} = |\delta_{\text{LR}}^q|_{ij} e^{i\theta}. \quad (40)$$

We firstly consider the case of $(\delta_{\text{LR}}^d)_{23} \neq 0$. The MIA parameter $(\delta_{\text{LR}}^d)_{23}$ dominates the gluino contribution to the Wilson coefficient $C_{7\gamma}(m_b)$, and therefore strong constraints on its magnitude, as listed in Table 2, can be derived by considering the data of $\text{Br}(B \rightarrow X_s \gamma)$. In numerical calculations, we assume $\tilde{m} = 500$ GeV, $x_{\tilde{g}} = 0.3, 1, 3$, and $\arg(\delta_{\text{LR}}^d)_{23} = 0, \pi/2$, and π , respectively. In Table 2, we also show the constraints on the magnitude of the parameter $(\delta_{\text{RL}}^d)_{23}$.

One can see from Table 2 that the upper bounds on $|(\delta_{\text{LR}}^d)_{23}|$ are sensitive to the phase of this mass insertion. But the phase of the parameter $(\delta_{\text{RL}}^d)_{23}$ is still a free parameter. Since the parameter $(\delta_{\text{RL}}^d)_{23}$ appears in $\tilde{C}_{7\gamma}(m_b)$ only, which does not mix with $C_{7\gamma}(m_b)$.

Table 2 Upper bounds on MIA parameters $|(\delta_{\text{LR}}^d)_{23}|$ and $|(\delta_{\text{RL}}^d)_{23}|$ from the data of $\text{Br}(B \rightarrow X_s \gamma)$ for $\tilde{m} = 500$ GeV, $x_{\tilde{g}} = 0.3, 1, 3$ and $\arg(\delta_{\text{LR}}^d)_{23} = 0$ (a), $\pi/2$ (b), and π (c), respectively.

x	0.3	1	3
	(a) 0.0027	(a) 0.0023	(a) 0.0013
$ (\delta_{\text{LR}}^d)_{23} $	(b) 0.0120	(b) 0.0120	(b) 0.0087
	(c) 0.0040	(c) 0.0033	(c) 0.0019
$ (\delta_{\text{RL}}^d)_{23} $	0.0102	0.0092	0.0059

[§]The term ‘‘real constraint’’ means the constraint of $|(\delta_{\text{AB}}^{u,d})_{ij}| \ll 1$.

3.2 One Mass Insertion: Chargino Contributions

Now we consider the chargino contribution as the dominant SUSY effect to $b \rightarrow s \gamma$. From Eqs. (37) and Eq. (38), one can see easily that the LL and LR sector mass insertions give the dominant contribution to the Wilson coefficients $C_{7\gamma}(m_b)$ and $\tilde{C}_{7\gamma}(m_b)$.

From the data of $\text{Br}(B \rightarrow X_s \gamma)$ as given in Eq. (34) and the requirement of an SM-like $C_{7\gamma}(m_b)$ as indicated by the measured branching ratios of $B \rightarrow X_s l^+ l^-$ decay, the upper bounds on $(\delta_{LL}^u)_{31,32}$ and $(\delta_{LR}^u)_{31,32}$ as functions of the gaugino mass M_2 are given in Table 3. In the numerical calculation, we use $\tilde{m} = 500$ GeV, $\mu = \pm 300$ GeV, and $\tan \beta = 20$. For larger values of $\tan \beta$, the upper bounds as listed in Table 3 will be scaled by a factor of $20/\tan \beta$.

Table 3 Upper bounds on $|(\delta_{LL}^u)_{31,32}|$ and $|(\delta_{LR}^u)_{31,32}|$ from the data of $\text{Br}(B \rightarrow X_s \gamma)$ and $\text{Br}(B \rightarrow X_s l^+ l^-)$ for $\tilde{m} = 500$ GeV, $\mu = 300$ GeV, $\tan \beta = 20$ and the phase $\theta = 0$ (a), $\pi/2$ (b), and π (c), respectively.

M_2	$\mu = 300$			$\mu = -300$		
	200	400	600	200	400	600
$ (\delta_{LL}^u)_{31} $	(a)0.222	(a)0.320	(a)0.440	(a)0.161	(a)0.231	(a)0.316
	(b)0.722	(b)1.028	(b)1.408	(b)0.662	(b)0.957	(b)1.319
	(c)0.154	(c)0.221	(c)0.305	(c)0.233	(c)0.333	(c)0.457
$ (\delta_{LL}^u)_{32} $	(a)0.049	(a)0.070	(a)0.097	(a)0.035	(a)0.051	(a)0.069
	(b)0.159	(b)0.226	(b)0.309	(b)0.145	(b)0.210	(b)0.290
	(c)0.034	(c)0.049	(c)0.067	(c)0.051	(c)0.073	(c)0.100
$ (\delta_{LR}^u)_{31} $	0.201	0.197	0.195	0.204	0.199	0.197
$ (\delta_{LR}^u)_{32} $	0.044	0.043	0.043	0.045	0.044	0.043

By taking into account the data of $\text{Br}(B \rightarrow X_s l^+ l^-)$, the constraints on the MIA parameters become more stronger than those obtained by considering the data of $\text{Br}(B \rightarrow X_s \gamma)$ only. In Figs. 1 and 2, we show the phase dependence of the bounds on $|(\delta_{LL}^u)_{31}|$ and $|(\delta_{LL}^u)_{32}|$ by assuming $M_2 = 200$ GeV, $\tilde{m} = 500$ GeV, $\mu = 300$ GeV, and $\tan \beta = 20$. Here both the shadow regions of A and B are allowed by the data of $\text{Br}(B \rightarrow X_s \gamma)$, but the region A is excluded by considering the additional restrictions coming from the data of $\text{Br}(B \rightarrow X_s l^+ l^-)$.

Table 4 Upper bounds on $|(\delta_{LL}^d)_{13,23}|$ obtained from Table 3 and Eqs. (42) and (43).

M_2	$\mu = 300$			$\mu = -300$		
	200	400	600	200	400	600
$ (\delta_{LL}^d)_{13} $	(a)0.211	(a)0.305	(a)0.419	(a)0.153	(a)0.220	(a)0.301
	(b)0.687	(b)0.978	(b)1.340	(b)0.630	(b)0.911	(b)1.255
	(c)0.147	(c)0.210	(c)0.290	(c)0.222	(c)0.317	(c)0.435
$ (\delta_{LL}^d)_{23} $	(a)0.098	(a)0.140	(a)0.194	(a)0.070	(a)0.102	(a)0.138
	(b)0.318	(b)0.452	(b)0.618	(b)0.290	(b)0.420	(b)0.580
	(c)0.068	(c)0.098	(c)0.134	(c)0.102	(c)0.146	(c)0.200

Furthermore, because of the SU(2) gauge invariance the soft scalar mass M_Q^2 is common for the up and down sectors. Therefore, one can get the following relations between the up and down type mass insertions:

$$(\delta_{LL}^d)_{ij} = [V_{\text{CKM}}^+(\delta_{LL}^u) V_{\text{CKM}}]_{ij}. \quad (41)$$

For the elements $ij = 31, 32$, we have

$$(\delta_{LL}^d)_{31} = (\delta_{LL}^u)_{31} - \lambda(\delta_{LL}^u)_{32} + \mathcal{O}(\lambda^2), \quad (42)$$

$$(\delta_{LL}^d)_{32} = (\delta_{LL}^u)_{32} + \lambda(\delta_{LL}^u)_{31} + \mathcal{O}(\lambda^2). \quad (43)$$

Consequently, the upper bounds on $|(\delta_{LL}^u)_{31,32}|$ can be conveyed to a constraint on $|(\delta_{LL}^d)_{31,32}|$, which equals $|(\delta_{LL}^d)_{13,23}|$, due to the hermiticity of $(M_D^2)_{LL}$. From the bounds as given in Table 3 and the relation in Eqs. (42) and (43), the upper bounds on $|(\delta_{LL}^d)_{13,23}|$ can be obtained, as listed in Table 4, where the terms proportional to λ^2 or higher powers

are neglected. These are the strongest constraints one may obtain on $|(\delta_{LL}^d)_{13,23}|$, and therefore it should be taken into account in analyzing the “LL” part of the gluino contribution to the $b \rightarrow s$ and $b \rightarrow d$ transitions.

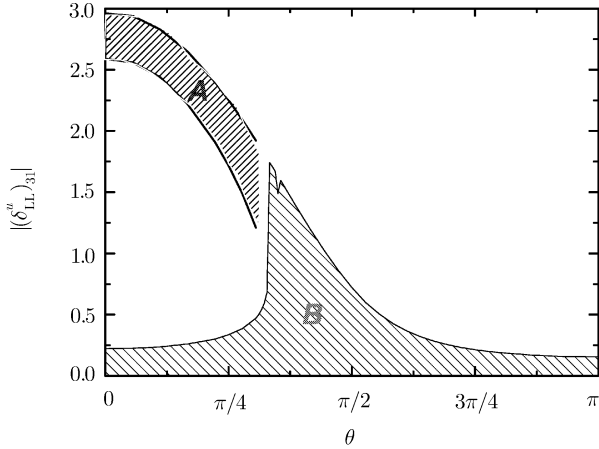


Fig. 1 Plot of $|(\delta_{LL}^u)_{31}|$ as a function of its phase θ . Here both A and B regions are allowed by the data of $\text{Br}(B \rightarrow X_s \gamma)$, but the region A is excluded by the requirement of an SM-like $C_{7\gamma}(m_b)$.

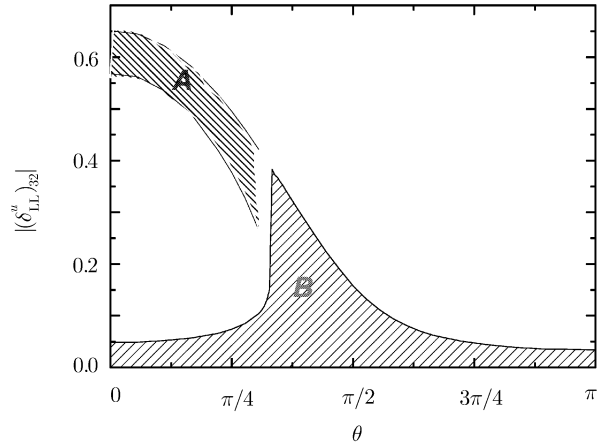


Fig. 2 Plot of $|(\delta_{LL}^u)_{32}|$ as a function of its phase θ . Here both A and B regions are allowed by the data of $\text{Br}(B \rightarrow X_s \gamma)$, but the region A is excluded by the requirement of an SM-like $C_{7\gamma}(m_b)$.

3.3 Two Mass Insertions

Finally we consider the scenario in which two mass insertion parameters are non-zero at a time. Because of the interference between different terms, the situation becomes more complicated than the cases of one mass insertions. By assuming $M_2 = 200$ GeV, $\tilde{m} = 500$ GeV, $x_{\tilde{g}} = 1$, and $\tan \beta = 20$, we consider only two typical cases:

Case 1 $(\delta_{LL}^u)_{32}$ and $(\delta_{LR}^u)_{23}$ in $C_{7\gamma}(m_b)$ are non-zero, i.e.

$$C_{7\gamma}(m_b) = -0.3052 - 17.41(\delta_{LR}^d)_{23} + 1.295(\delta_{LL}^u)_{32}, \quad \tilde{C}_{7\gamma}(m_b) = 0. \quad (44)$$

Case 2 $(\delta_{RL}^d)_{23}$ and $\delta_{LR}^u)_{32}$ in $\tilde{C}_{7\gamma}(m_b)$ are non-zero, i.e.

$$C_{7\gamma}(m_b) = -0.3052, \quad \tilde{C}_{7\gamma}(m_b) = -17.41(\delta_{RL}^d)_{23} + 3.601(\delta_{LR}^u)_{32}. \quad (45)$$

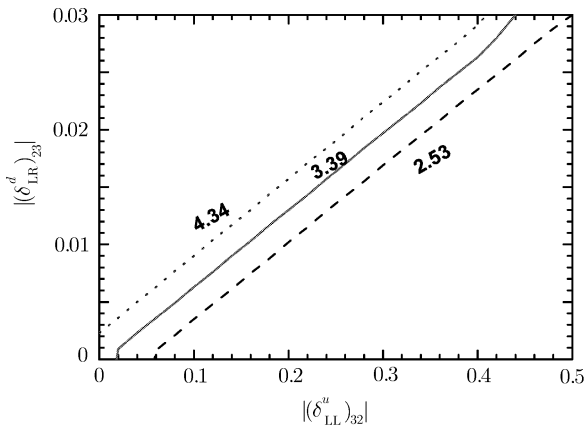


Fig. 3 Contour plot of $\text{Br}(B \rightarrow X_s \gamma) \times 10^4$ as a function of $|(\delta_{LL}^u)_{32}|$ and $|(\delta_{LR}^d)_{23}|$ with the same zero phase.

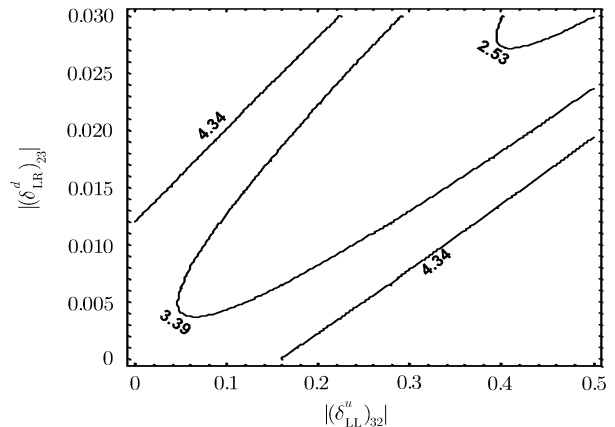


Fig. 4 Contour plot of $\text{Br}(B \rightarrow X_s \gamma) \times 10^4$ as a function of $|(\delta_{LL}^u)_{32}|$ and $|(\delta_{LR}^d)_{23}|$ with the same phase of $\theta = \pi/2$.

We firstly consider Case 1, where the SM and the chargino contributions are taken into account. In Fig. 3, we show the contour plot of $\text{Br}(B \rightarrow X_s \gamma)$ (in unit of 10^{-4}) as a function of $|(\delta_{LL}^u)_{32}|$ and $|(\delta_{LR}^d)_{23}|$ with the same zero phase. In Fig. 3, the dashed and dotted line show the lower and upper bounds of the branching ratios as given in Eq. (34): $2.53 \times 10^{-4} \leq \text{Br}(B \rightarrow X_s \gamma) \leq 4.34 \times 10^{-4}$, while the solid line refers to the central value of the data. The region between the dotted and dashed lines are allowed by the data of both $B \rightarrow X_s \gamma$ and $B \rightarrow X_s l^+ l^-$ decay. Figure 4

shows the same contour plot as Fig. 3, but for a non-zero phase of $\theta = \pi/2$.

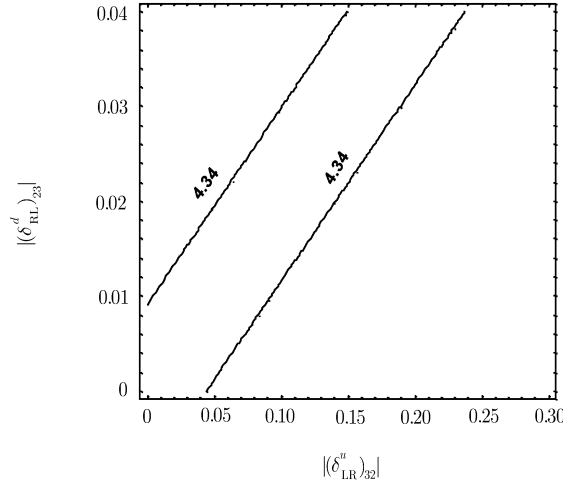


Fig. 5 Contour plot of $\text{Br}(B \rightarrow X_s \gamma) \times 10^4$ as a function of $|\delta_{\text{LR}}^u{}_{32}|$ and $|\delta_{\text{RL}}^d{}_{23}|$ with the same zero phase.

We now consider Case 2, where the SM and the gluino contributions are taken into account. In Fig. 5, we show the contour plot of $\text{Br}(B \rightarrow X_s \gamma)$ (in unit of 10^{-4}) as a function of $|\delta_{\text{LR}}^u{}_{32}|$ and $|\delta_{\text{RL}}^d{}_{23}|$ with the same zero phase. The region between the dotted and solid lines are allowed by the data of both $B \rightarrow X_s \gamma$ and $B \rightarrow X_s l^+ l^-$ decay.

4 Summary

In this paper, by comparing the theoretical predictions with the corresponding measured branching ratios of $B \rightarrow X_s \gamma$ and $B \rightarrow X_s l^+ l^-$ decays, we make an update for the upper bounds on the mass insertions parameters $(\delta_{\text{AB}}^{u,d})_{ij}$ appeared in the MSSM.

From the well-measured $B \rightarrow X_s \gamma$ decays, the strong constraints on the MIA parameters can be obtained. From the latest Belle and BaBar measurements of the inclusive $B \rightarrow X_s l^+ l^-$ branching ratios, one gets to know that an SM-like (negative) $C_{7\gamma}(m_b)$ is favored, and therefore further constraints on the MIA parameters can be derived. We found that the information from the measured branching ratio of $B \rightarrow X_s l^+ l^-$ decay can help us to improve the upper bounds on the mass insertions parameters $(\delta_{\text{AB}}^g)_{3j,i3}$ in the MSSM.

We focus on the possible large new physics contributions to the Wilson coefficients $C_{7\gamma,8g}$ and $\tilde{C}_{7\gamma,8g}$ coming from chargino and gluino penguin diagrams. Throughout our analysis, the SM contributions are always taken into account. From the numerical calculations, we found the following points

1. In the one mass insertion approximation, strong upper bounds on the mass insertion parameters $(\delta_{\text{LL}}^u)_{31,32}$, $(\delta_{\text{LL}}^d)_{13,23}$, $(\delta_{\text{LR}}^d)_{23}$, $(\delta_{\text{LR}}^u)_{31,32}$, and $(\delta_{\text{RL}}^d)_{23}$ are obtained, as collected in Tables 2 ~ 4.
2. As shown explicitly in Figs. 1 and 2, the region A allowed by the data of $\text{Br}(B \rightarrow X_s \gamma)$ is excluded by the requirement of an SM-like $C_{7\gamma}(m_b)$ imposed by the data of $\text{Br}(B \rightarrow X_s l^+ l^-)$.
3. Under two-mass insertion approximation, strong upper bounds on $(\delta_{\text{LL}}^u)_{32}$, and $(\delta_{\text{LR}}^d)_{23}$, and $(\delta_{\text{LR}}^u)_{32}$ and $(\delta_{\text{RL}}^d)_{23}$ can also be obtained, as shown in Figs. 3 ~ 5.

References

- [1] A. Djouadi, *et al.*, hep-ph/9901246.
- [2] L.J. Hall, E.A. Kostelevy, and S. Raby, Nucl. Phys. B **267** (1986) 415; J.S. Hagelin, S. Kelley, and T. Tanaka, **415** (1994) 293; E. Gabrielli, A. Masiero, and L. Silvestrini, Phys. Lett. B **374** (1996) 80.
- [3] F. Gabbiani, E. Gabrielli, A. Masiero, and L. Silvestrini, Nucl. Phys. B **477** (1996) 321.
- [4] S. Khalil, Phys. Rev. D **72** (2005) 035007.
- [5] S. Khalil and E. Kou, Phys. Rev. Lett. **91** (2003) 241602; D. Chakraverty, E. Gabrielli, K. Huitu, and S. Khalil, Phys. Rev. D **68** (2003) 095004; P. Ball, S. Khalil, and

- E. Kou, Phys. Rev. D **69** (2004) 115011; S. Khalil and E. Kou, Phys. Rev. D **71** (2004) 114016; S. Abel and S. Khalil, Phys. Lett. B **618** (2005) 201; S. Khalil, Phys. Rev. D **72** (2005) 055020.
- [6] E. Gabrielli, K. Huitu, and S. Khalil, Nucl. Phys. B **710** (2005) 139.
- [7] Heavy Flavor Averaging Group,
<http://www.slac.stanford.edu/xorg/hfag>;
- [8] P. Gambino and M. Misiak, Nucl. Phys. B **611** (2001) 338; A.J. Buras, A. Czarnecki, M. Misiak, and J. Urban, Nucl. Phys. B **631** (2002) 219.
- [9] C. Bobeth, P. Gambino, M. Gorbahn, and U. Haisch, J. High. Energy Phys. **04** (2004) 071; A. Ghinculov, T. Hurth, G. Isidori, and Y.P. Yao, Nucl. Phys. B **685** (2004) 351.
- [10] P. Gambino, U. Haisch, and M. Misiak, Phys. Rev. Lett. **94** (2005) 061803.
- [11] T. Hurth, hep-ph/0511280; Z.J. Xiao, C.S. Li, and Kuang-Ta Chao, Phys. Rev. D **64** (2000) 094008; *ibid.* **63** (2001) 074005; Zhen-Jun Xiao and Wen-Juan Zou, Phys. Rev. D **70** (2004) 094008; Wen-Juan Zou and Zhen-Jun Xiao, Phys. Rev. D **72** (2005) 094026.
- [12] G. Buchalla, A.J. Buras, and M.E. Lautenbacher, Rev. Mod. Phys. **68** (1996) 1125.
- [13] M. Kobayashi and T. Maskawa, Prog. Theor. Phys. **49** (1973) 652.
- [14] F.M. Borzumati and C. Greub, Phys. Rev. D **58** (1998) 074004; *ibid.* **59** (1999) 057501.
- [15] Z.J. Xiao and L.B. Guo, Phys. Rev. D **69** (2004) 014002.
- [16] K. Chetyrkin, M. Misiak, and M. Munz, Phys. Lett. B **400** (1997) 206; **425** (1998) 414(E); A.J. Buras, A. Kwiatkowski, and N. Pott, Phys. Lett. B **414** (1997) 157; C. Greub and T. Hurth, Phys. Rev. D **54** (1996) 3350; *ibid.* **56** (1997) 2934.
- [17] A.F. Falk, M. Luke, and M. Savage, Phys. Rev. D **49** (1994) 3367.
- [18] M.B. Voloshin, Phys. Lett. B **397** (1997) 275; A. Khodjamirian, R. Ruckl, G. Stoll, and D. Wyler, Phys. Lett. B **402** (1997) 167; Z. Ligeti, L. Randall, and M.B. Wise, Phys. Lett. B **402** (1997) 178; A.K. Grant, A.G. Morgan, S. Nussinov, and R.D. Peccei, Phys. Rev. D **56** (1997) 3151.
- [19] S. Bertolini, F. Borzumati, A. Masiero, and G. Ridolfi, Nucl. Phys. B **353** (1995) 591.
- [20] E. Gabrielli and G.F. Giudice, Nucl. Phys. B **433** (1995) 3.